

Model-based correction for brain shift in deep brain stimulation burr hole procedures: a comparison using interventional magnetic resonance imaging

Ma Luo*^a, Saramati Narasimhan^a, Alastair J. Martin^b, Paul S. Larson^c, Michael I. Miga^{a,d,e,f}

^aDepartment of Biomedical Engineering, Vanderbilt University, Nashville, TN

^bDepartment of Radiology and Biomedical Imaging, University of California, San Francisco, CA

^cDepartment of Neurological Surgery, University of California, San Francisco, CA

^dDepartment of Neurological Surgery, Vanderbilt University Medical Center, Nashville, TN

^eDepartment of Radiology, Vanderbilt University Medical Center, Nashville, TN

^fVanderbilt Institute for Surgery and Engineering, Vanderbilt University, Nashville, TN

ABSTRACT

Deep brain stimulation (DBS) is an effective treatment for movement disorders, e.g. Parkinson's disease. The quality of DBS treatment is dependent on the implantation accuracy of DBS electrode leads into target structures. However, brain shift during burr hole procedures has been documented and hypothesized to negatively impact treatment quality. Several approaches have been proposed to compensate for brain shift in DBS, namely microelectrode recording (MER) and interventional magnetic resonance (iMR) imaging. Though both demonstrate benefits in guiding accurate electrode placement, they suffer drawbacks such as prolonged procedures and in the latter, cost considerations. Hence, we are exploring a model-based brain shift compensation strategy in DBS to improve targeting accuracy for surgical navigation. Our method is a deformation-atlas-based approach, i.e. potential intraoperative deformations are pre-computed via biomechanical model under varying conditions, combined with an inverse problem driven by sparse intraoperative data for estimating volumetric brain deformations. In this preliminary feasibility study, we examine our model's ability to predict brain shift in DBS by comparing with iMR in one patient. The evaluation includes: (1) a subsurface deformation comparison where subsurface shifts measured by iMR are compared to model-predicted counterparts; (2) a second comparison at surgical targets where the atlas-method is compared to deformations measured by non-rigid image-to-image registration using preoperative image and iMR. For the former, the model reduces alignment error from 8.6 ± 1.4 to 3.6 ± 0.8 mm, representing ~58.6% correction. For the latter, model estimated brain shifts at surgical targets are 2.4 and 0.6 mm, consistent with clinical observations.

Keywords: Brain shift, deep brain stimulation, neurosurgery, finite element, computational modeling

1. INTRODUCTION

Movement disorders, such as Parkinson's disease (PD), essential tremor and dystonia can have devastating effects on the quality of life of patients, as well as negative impacts on the productivity and well-being of society^{1,2}. PD, for example, impacts 0.3% of the general population and 1-2% of people over age 60; one third of PD patients lose employment within a year, and a majority lose full-time employment within 5 years². Deep brain stimulation (DBS) has emerged as an important and effective surgical therapy for patients with these movement disorders^{1,2}. A 2013 review by Deuschl et al. analyzed 6 clinical studies to examine the treatment outcome of DBS in PD patients when targeting the subthalamic nucleus (STN), and all these studies demonstrated a significant motor symptom reduction varying from 28.6% to 52% when comparing patients' post-operative condition with stimulation-on/medication-off to their medication-off condition prior to surgery as measured by the Unified Parkinson's Disease Rating Scale (UPDRS) part III³.

Therapeutically, DBS delivers electrical pulses continuously to a targeted brain structure such as STN via implanted electrodes that are connected to an internalized stimulator, which is programmable in pulse width, frequency

and amplitude^{1,4}. Though the underlying mechanism for its therapeutic effectiveness continues to be debated, it is hypothesized that DBS induces the regularization of neuronal patterns by modulating neural signaling within the target^{2,3,5}. This regularization is hypothesized to introduce cumulative local effects on a larger neural network resulting in disease symptom reduction^{2,3,5}.

Critical to the success of DBS is the accurate surgical targeting and electrode implantation⁶⁻⁸. The therapeutic benefit of DBS however is negatively impacted when inaccurate targeting occurs due to brain shift, or soft tissue deformation, during burr hole procedures. Specifically, when the assumption that brain tissue remains rigid and experiences no movement between preoperative imaging data and intraoperative patient anatomy is compromised due to brain shift, suboptimal targeting and consequently therapy may ensue^{9,10}. The impacts of inaccurate targeting are short- and long-term symptom management, inadequate benefits, difficulty with device programming, and potential adverse events¹¹. Specifically, a study by Balachandran et al. suggests that if the electrode is placed 3-4 mm away from the target, the stimulation may become ineffective due to (1) failure to stimulate the desired neuronal groups, or (2) introduction of adverse effects when undesired areas are stimulated, or (3) the need for higher currents to produce the desired treatment, which can lead to poor battery life¹². The potential negative impact of brain shift requires careful consideration especially given that the size of STN is approximately 6 mm × 4 mm × 5 mm, and the electrode contacts of the DBS lead are merely 1.5 mm in length and separated by 0.5 or 1.5 mm^{12,13}.

Several studies have observed and reported brain shift in DBS burr hole procedures. Winkler et al. reported brain movement of 2 mm in the target region of STN¹⁴. Similarly, Miyagi et al. reported electrode target dislocation up to 2.3 mm¹⁵. Khan et al. found shift of similar magnitudes in deep brain structures and reported average displacements of 1.8 mm and 1.6 mm in anterior commissure (AC) and posterior commissure (PC), respectively⁹. Elias et al. also found 7.6% of 66 patients studied experienced shift at the AC over 2 mm; additionally, the study found the largest average displacements were in the front cortex at levels of 3.5 mm¹⁶. A recent study by Ivan et al. with 44 patients found shift ranging from 0.0-10.1 mm, with the greatest shift occurring in the frontal lobe; 9% of patients experienced shift over 2 mm in deep brain structures while 20% had 1 to 2 mm shifts in deep structures¹⁰. In traditional DBS lead implantation procedures, one strategy to overcome brain shift is to use microelectrode recordings (MER) to map and delineate the target region⁸. However, while a commonly used technique, the challenges of the MER approach are numerous: (1) the requirement of patient participation in an awake procedure, which requires the patients to be off medications^{8,17}; (2) the possibility of multiple electrode passes to optimize lead placement, which can potentially lead to a higher risk of intracranial bleeding and other potential adverse complications^{8,17,18}; and (3) MER requires special equipment and expertise, significant training, as well as dedicated intraoperative time prolonging operating duration, which can potentially lead to additional risks and complications^{19,20}. To address these shortcomings of MER, interventional MR (iMR) has also been introduced for DBS implantations. The advantage of employing iMR is that by performing the implantation procedure entirely within the MRI scanner, the target structures can be visualized with direct imaging, thus monitoring and accounting for intraoperative brain shift; furthermore, iMR reduces the number of brain penetrations needed^{6,17}. Lastly, as a real-time direct imaging method, iMR-guided DBS procedures are performed with patients under general anesthesia, thus the patients may remain on their medications^{6,17}. While iMR provides an alternative approach to MER in compensating brain shift and guiding accurate electrode placement, its cost, training, and encumbrance are considerations for medical centers. Therefore, a cost-effective and workflow-friendly model-based brain shift correction strategy, if accurate, would be a desirable alternative. The study reported herein presents preliminary steps examining the feasibility of using a model-based approach to predict intraoperative brain shift in DBS procedures with only sparse intraoperative data. In this study, the model's ability to account for brain shift is evaluated and compared with iMR data.

2. METHODOLOGY

2.1 Overview

This preliminary feasibility study has two objectives: (1) evaluation of the performance of our model-based brain shift correction strategy in recovering subsurface shift in DBS procedures; (2) brain shift estimation at intended surgical targets. Preoperative and intraoperative MR images of one patient were acquired at University of California, San Francisco (UCSF) with IRB approval. The size of the preoperative MR image volume of the patient was 240×240×85 with voxel spacing of (1.00, 1.00, 2.00) mm; for the intraoperative MR image volume, the size was 256×256×107 and voxel spacing was (1.02, 1.02, 1.50) mm.

2.2 Finite Element Model Construction and Boundary Condition Assignment

The brain volume was manually segmented from the preoperative MR image volume; subsequently, a surface was extracted from the segmented brain via a marching cubes algorithm, followed by a surface smoothing step. With the surface mesh established, a custom-build mesh generator was employed to generate a 3D volumetric tetrahedral mesh, shown in Fig 1²¹.

Boundary conditions, specifically displacement and pressure conditions, are assigned based on a protocol developed and tested in our previous studies with modifications made to adapt to the unique nature of shift observed in DBS²²⁻²⁴. Two types of brain deformation were simulated in this study: gravity-induced shift and pneumoencephalic-induced shift. Briefly, the brain stem region was assigned fixed Dirichlet displacement boundary condition, and no drainage was permitted, i.e. a pure Neumann pressure boundary condition. Internal structures of the brain, namely falx cerebri and tentorium cerebelli, were given slip condition (i.e. tangential movement was permitted yet displacement in the normal-to-septa direction was not allowed) and similarly no drainage was allowed. The ventricle region was assigned to be stress free (i.e. free to deform) and at a fixed Dirichlet pressure boundary condition, representing a constant ventricular pressure. The remaining brain surface did not allow drainage out of the parenchyma. The displacement conditions of the remaining brain surface were determined by computing the dot product of the nodal normal and the gravitational vector at a given patient orientation (e.g. supine in iMR-guided DBS procedure). If the dot product is greater than a scalar tolerance set by the user, the particular node was given a boundary condition allowing slip. If the dot product was less than the scalar tolerance, the node was prescribed a stress free condition in gravity-induced shift. With respect to our novel pneumoencephalic-induced shift boundary condition, stresses were prescribed to these particular nodes on the surface in the normal direction to simulate the effect of air invasion pressing on brain tissue during the burr hole procedure. The inclusion of internal structures such as the falx and tentorium in our boundary condition description have shown to provide shift predictions that are more consistent with clinical observations²⁴.

We should note that the identification of the brain stem, falx, and tentorium structures is part of a fully automatic process previously reported^{23, 25-27}. Briefly an expert atlas image volume was segmented. The atlas volume was then rigidly and nonrigidly aligned to the patient's imaging volume. Subsequently the rigid and non-rigid transformations were applied to the brain stem, falx and tentorium segmented from the atlas image volume to obtain patient-specific representations of these structures in patient space^{25, 26}. The patient-specific brain mesh with the aforementioned internal structures is shown in Fig 1.

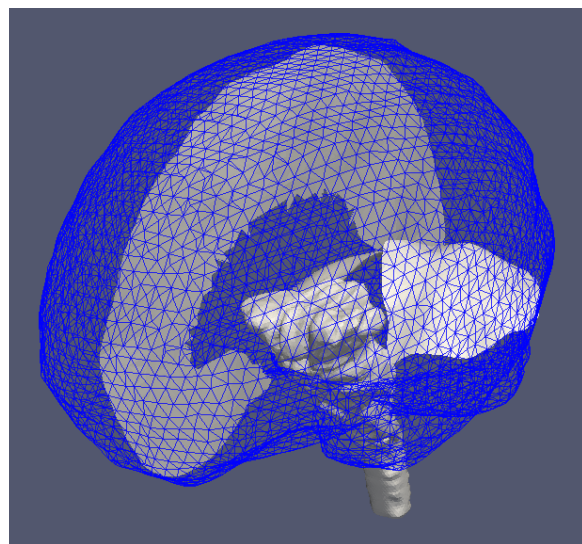


Figure 1. Patient-specific brain mesh with atlas falx cerebri, tentorium cerebelli, and brain stem registered to patient space by applying rigid and non-rigid image registrations.

2.3 Preoperative Computation – Deformation Atlas

Our model-based brain shift correction strategy constructs a suite of potential deformation solutions, forming a so-called ‘deformation atlas,’ based on numerous surgical variables. Previous studies have suggested that CSF loss precipitating brain sag in the direction of gravity may be a significant contributor of brain shift in DBS burr hole procedures^{9, 18, 28}. We therefore have modified our methodology from our previous brain shift correction model implementations (e.g. in Sun et al.²³) to simulate this gravity-induced shift. Furthermore, in our biphasic biomechanical model, which is detailed in Miga et al.²⁹, the impact of gravity and CSF loss is closely related— intraoperative CSF loss decreases the buoyancy, thus causing the brain to sag due to gravity. To accommodate the unpredictability of the surgical environment, and particularly asymmetric shift nature in DBS procedures, we simulated asymmetric CSF drainage on either side of the brain. We hypothesize that, given these are only burr hole interventions, a great deal of the natural compartmentalization of the brain

is maintained, which allows for some regions to preferentially lose CSF while others are not compromised and maintain fluid levels. Different CSF drainage configurations are shown in the top row of Fig 2, where blue represents the simulated CSF level in which the tissue weight and buoyancy forces are in equilibrium.

For pneumoencephalic-induced shift, the user specified dot product threshold described in Sec 2. 2 was varied, which modified the boundary nodes experiencing prescribed normal stress, in order to simulate different possible extents of air invasion and their corresponding impacts on the brain tissue.

For each unique set of these boundary conditions, partial differential equations associated with the biomechanics of brain deformation were resolved via the Galerkin Weighted Residual Method for a full volumetric brain deformation solution³⁰. Detailed derivation of the formulation and solution can be found in prior publications^{29, 31}. All of the distinct brain deformation solutions associated with each boundary condition set thus form the ‘deformation atlas.’ Examples of possible deformation solutions are shown in the bottom row of Fig 2, where white translucent surface is the preoperative configuration of the brain, and yellow surface represents model deformed solution, i.e. predicted gravity-induced deformation with boundary conditions depicted previously. Here it is worth noting our model’s ability to provide asymmetric shifts.

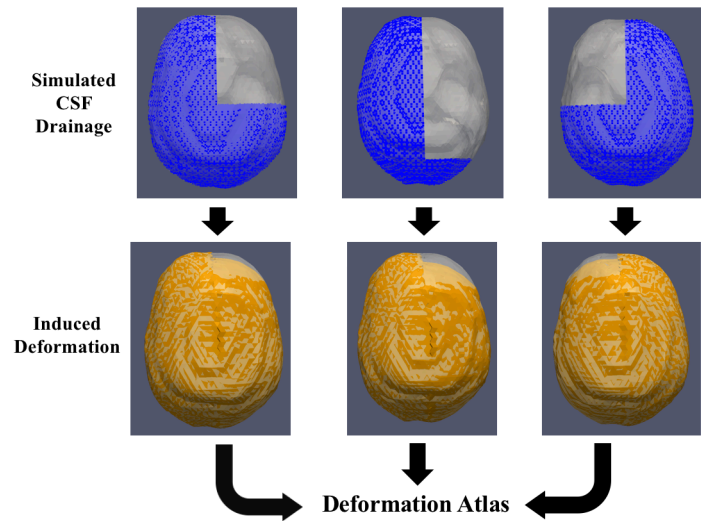


Figure 2. Top: Different CSF drainage levels simulated where blue represent the brain tissue submerged in CSF with different asymmetric drainage configurations on either side of the brain. Bottom: Gravity induced deformation predicted by the model resulting from different CSF drainage considerations, where white semi-transparent mesh is the preoperative mesh and the yellow mesh is the model predicted volumetric deformation based on corresponding CSF conditions simulated.

Examples of possible deformation solutions are shown in the bottom row of Fig 2, where white translucent surface is the preoperative configuration of the brain, and yellow surface represents model deformed solution, i.e. predicted gravity-induced deformation with boundary conditions depicted previously. Here it is worth noting our model’s ability to provide asymmetric shifts.

2.4 Inverse Problem

The patient iMR imaging volume was rigidly registered to the preoperative imaging volume via normalized mutual information²⁵. The quality of this registration was examined by fusing the two images shown in Fig 3 using Analyze 9.0 (AnalyzeDirect, Overland Park, KS), where Fig 3(A) and (B) show a slice of the preoperative and registered intraoperative images, and the Fig 3(C) is the difference image when the two images are fused. The fused image showed similar far field features, while noted quite significant brain shift in the front lobe and shape change occurring at the ventricle. Additionally, it is worth noting that this patient underwent a bilateral implantation, which can be observed on the registered intraoperative MR image or Fig 3(B).

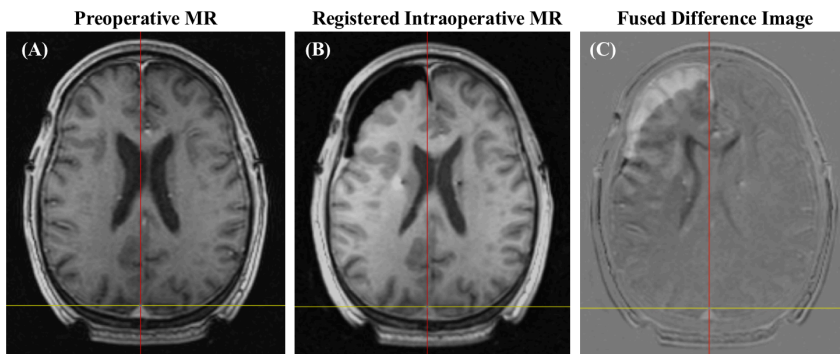


Figure 3. (A) A slice of preoperative MR image; (B) the corresponding slice on the registered intraoperative MR image; (C) fused difference image of preoperative and registered intraoperative MR images, noting brain shift in the frontal lobe, as well as shape change of the lateral ventricle.

With respect to the sparse data driving the non-rigid biophysical registration, homologous surface points were manually designated on the preoperative image and the registered intraoperative image using 3D Slicer shown in Fig 4³². These corresponding sparse surface points provided measurement of intraoperative surface deformation that was used to constrain the inverse problem. The number of surface points used to drive the model in this study was $n = 15$. The objective function associated with the inverse problem was to minimize the least squared error between the measured surface shift and predicted surface shift, shown in Eq (1):

$$\min \|Mw - u\|^2 \quad \exists w_i \geq 0 \text{ and } \sum_{i=1}^m w_i \leq 1 \quad (1)$$

where M is the deformation atlas associated with the designated cortical surface nodes, w are the combinatory coefficients, and u are the measured displacements. Once the optimal coefficients of the linear combination were determined, the coefficients were used to estimate a full volumetric intraoperative brain shift. Subsequently, the preoperative MR image was updated according to this deformation field via trilinear interpolation.

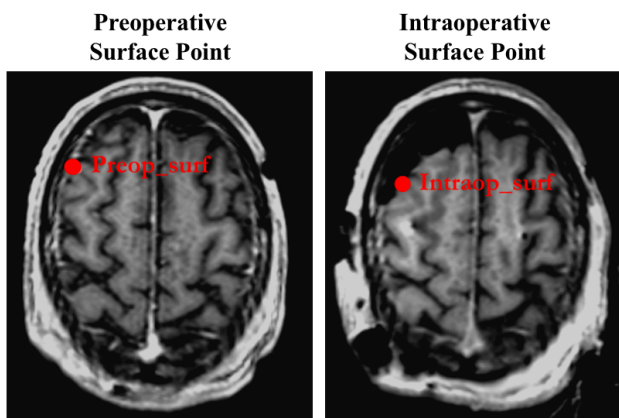


Figure 4. Corresponding surface feature points designated on preoperative MR image (left) and registered intraoperative MR image (right).

2.5 Evaluation of Subsurface Shift Recovery

To examine the model's ability to predict subsurface brain shift, homologous subsurface points were designated on the preoperative and registered intraoperative MR images using 3D Slicer³², a pair of such homologous subsurface targets is shown in Fig 5. The homologous subsurface points provided measurements of subsurface deformation that could be used as a ground truth comparator of our model-reconstructed values.

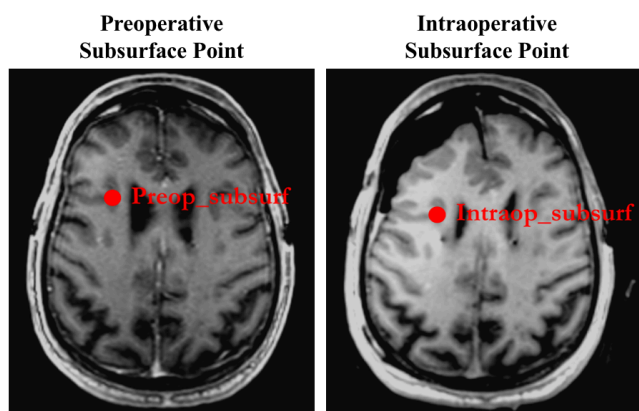


Figure 5. Corresponding subsurface feature points designated on preoperative MR image (left) and registered intraoperative MR image (right)

The performance of the model is assessed by two metrics, residual error and percent correction. Residual error, e , is the difference between measured subsurface deformation and its model predicted counterpart:

$$e = \|\vec{u}_{\text{error}}\| = \|\vec{u}_{\text{predicted}} - \vec{u}_{\text{measured}}\| \quad (2)$$

where \vec{u} is displacement or shift vector and $\|\cdot\|$ represents the L2 norm of the vector.

The quality of the brain shift correction is also evaluated by percent correction in Eq (3):

$$\text{Percent correction} = \left(1 - \frac{e}{\|\vec{u}_{\text{measured}}\|}\right) \times 100\% \quad (3)$$

2.6 Estimation of Surgical Target Shift

Since no surgical targets were designated on the preoperative image, the most distal ends of the electrode leads were identified on the registered intraoperative image and were assumed to be the intended surgical targets. With the knowledge of the location of the surgical targets on the intraoperative image, as well as a model-predicted deformation field generated from the inverse problem, displacement experienced by the surgical targets on the registered intraoperative image can be interpolated. By applying this interpolated displacement in the reverse direction, the location of the surgical targets can be mapped and estimated in the preoperative imaging space. With estimated target location on preoperative image and identified target location on registered intraoperative image, the shift at the intended surgical targets can be computed. To study the displacement of predicted surgical targets unbiasedly, for comparison purposes, the same procedure was carried out using deformation fields generated by non-rigidly registering the preoperative MR image to intraoperative MR image via two different non-rigid image registration techniques, namely ABA and Demon's algorithm^{26,33}.

3. RESULTS

The impact of volumetric deformation introduced by the model-based approach is shown in Fig 6, where intraoperative brain shift may be observed from the preoperative mesh (semi-white transparent) to the intraoperative mesh (red) in Fig 6(A), and the model's effort to compensate for such shift is shown in the comparison between the intraoperative mesh (red) and model prediction (blue) in Fig 6(B). Similarly, the model (blue nodes) is able to recover the ventricle shape change from preoperative (white) to intraoperative (red) state to some degree illustrated in Fig 6(C) and (D).

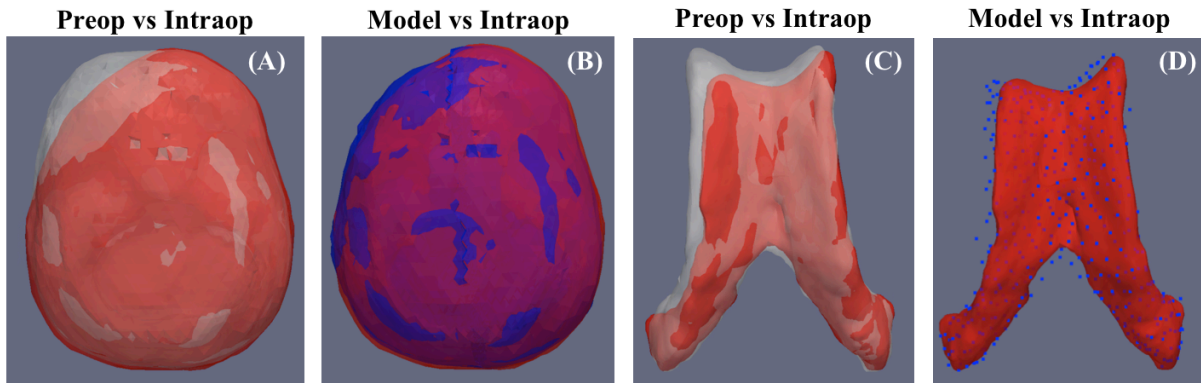


Figure 6. (A) Comparison between preoperative (white semi-transparent) brain mesh and intraoperative (red) brain mesh; (B) comparison between intraoperative (red) brain mesh and model predicted (blue) brain mesh; (C) comparison between preoperative (white semi-transparent) and intraoperative (red) lateral ventricle; (D) comparison between intraoperative (red) and model predicted (blue) lateral ventricle.

Quantitatively, for subsurface targets, i.e. corresponding subsurface points selected on preoperative and rigidly registered intraoperative images, the average measured subsurface deformation is 8.6 ± 1.4 mm [n=16]. Using our model correction method, this alignment error was reduced to 3.6 ± 0.8 mm, representing approximately 58.6% correction. A comparison of the measured subsurface deformation and corresponding model prediction is shown in Fig 7, where the red vectors are measured shift, and the blue vectors are their model predicted counterparts.

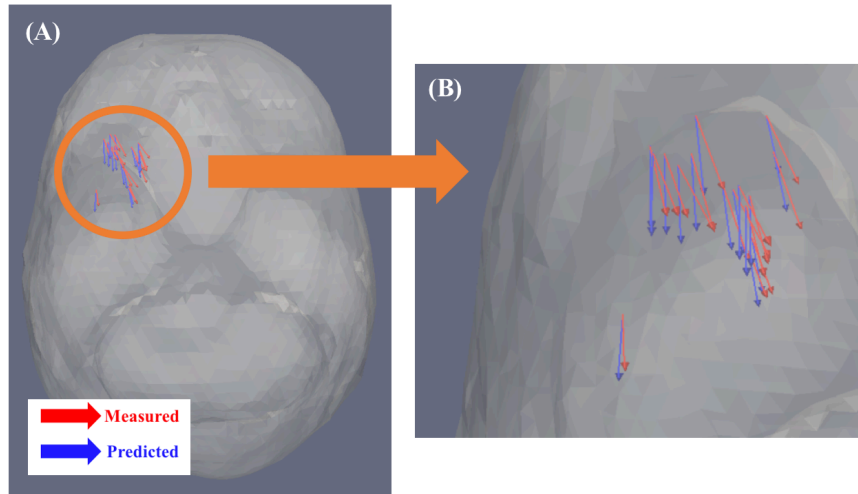


Figure 7. (A) Comparison between measured subsurface displacement (red vectors) and model predicted subsurface displacement (blue); (B) a zoomed view of the measured displacement (red) and model prediction (blue)

In addition to assessing our model’s ability to compensate for subsurface shift, we are particularly interested in understanding shift at surgical targets associated with DBS therapy in deep brain structure. From literature, these targets only shift on the order of 1-2 voxels. While electrode position is easy to discern in the intraoperative image set, finding the corresponding target in the preoperative image is difficult with our current data. Thus, brain shift at the intended surgical targets was examined using deformation fields generated from model prediction and two non-rigid image registration techniques (ABA and Demon’s) ^{26, 33} and compared as outlined in Sec 2.6. The displacements at surgical targets as predicted by three methods are shown in Table 1. The displacement results suggest that an average of approximately 2 mm shift is estimated at the surgical target location, which is consistent with clinical observations as well as prior publications. We should note that while data in Table 1 represent magnitude similarities, the directionality of shift prediction, i.e. ultimate electrode targeting location is different among methods. The similarity in magnitudes should not be regarded as a similarity of preoperative target location. This discrepancy in the predicted directionality among methods will be discussed further in Sec 4.

Table 1. Estimated shift at surgical targets predicted by model-based approach, and two non-rigid image registration techniques, ABA and Demon’s algorithms

	Right target (mm)	Left target (mm)	Average (mm)
Model	0.6	2.4	1.5
ABA	1.7	3.3	2.5
Demon’s	1.5	3.6	2.6
Average (mm)	1.3	3.1	2.2

4. DISCUSSION

The results of this preliminary feasibility study indicate that the developed model-based deformation-atlas approach to account for intraoperative brain shift has the potential to become a viable option for assisting surgical navigation and

accurate targeting in DBS burr hole procedures. The brain shift correction algorithm is able to reduce alignment error from 8.6 ± 1.4 mm to 3.6 ± 0.8 mm, representing approximately 58.6% correction. Qualitatively, the model's ability to compensate for intraoperative brain shift may be observed in Fig 6, where the model was able to capture some of the soft tissue deformation experienced between the patient's preoperative to intraoperative state on the surface, evident in comparing model predicted brain mesh with intraoperative brain mesh, as well as subsurface, evident in comparing model predicted lateral ventricle with its intraoperative counterpart. Additionally, when using the deformation field derived from the model prediction, the shifts at left and right surgical targets are estimated to be 2.4 and 0.6 mm, respectively. These magnitudes are consistent with prior studies and may impact treatment outcome negatively if not appropriately corrected. Although promising, our experience points to the need for refinements and improvements in both our brain shift correction model as well as the feasibility study design.

There are several aspects of this study that can be improved. First of all, from Fig 6 and Fig 7, it is apparent that while the model is able to compensate some intraoperative brain shift, its performance in medial-lateral direction (left-right in these figures) is less satisfying, producing mismatches between intraoperative measurement (red) and model prediction (blue). When further analyzing the subsurface targets and breaking the measured shift and residual error into individual components, we found for measured shift that 17.3% is in medial-lateral direction, 66.5% is in anterior-posterior direction, and 16.1% is in superior-inferior direction. In regards to the error or \vec{u}_{error} in Eq (2) after model correction: 58.3% of error is in medial-lateral direction, 16.9% in anterior-posterior, and 24.9% in superior-inferior. This suggests that our model in its current implementation, with the patient in the supine position or gravity in anterior-posterior direction, has some difficulty recovering components of lateral shift, especially in the medial-lateral direction. Refinement of the model to better account for these lateral shift components is necessary to enhance the accuracy of our model-based approach and ensure treatment outcome, since the residual error after our model correction (3.6 mm) is still relatively significant for accurate surgical navigation and targeting. An interesting finding from performing the subsurface shift component analysis is that the majority of our measured shift (66.5%) is in the direction of gravity or anterior-posterior direction, and this is consistent with the reporting of many previous studies^{9, 10, 15, 34}.

Secondly, although designed to be a feasibility study, we recognize that the use of surface data is not likely to be available in a clinical DBS procedure without intraoperative imaging. The availability and accessibility of the data on the cortical surface is limited for typical burr hole procedures. For our model-based approach to be clinically applicable, intraoperative imaging techniques such as computed tomography (CT) and/or ultrasound (US) may be employed as means to acquire sparse intraoperative data that can be used to drive the deformation-atlas model. Nevertheless, it is encouraging that the results of this study suggest that limited and sparse intraoperative information, surface and/or subsurface, may be utilized in our model-based correction framework to reduce alignment error introduced by brain shift even in the challenging case of asymmetric shift as shown here.

Furthermore, as preliminary and exploratory steps, the sample size in this study is limited with respect to the analysis of one patient and the number of subsurface targets. In the future, we would like to expand the sample size, both in the number of patients and the number of subsurface targets examined, to gain a better understanding of the model's ability to capture brain shift in DBS burr hole procedures. Additionally, most subsurface targets examined here are in the frontal lobe as they experience larger shifts, as noted by several studies^{10, 16, 35}, and can be easily identified on the MR images with high fidelity. Low shift targets, on the other hand, are more difficult to discern on MR images and more vulnerable to partial volume effects as well as human errors such as landmark identifications in selecting homologous surface and subsurface targets. Although challenging, shift studies that incorporate both low and high shift scenarios, and with respect to DBS targets such as the STN, are important to conduct to enable a more comprehensive understanding of the model's ability to predict intraoperative deformations.

Lastly, as noted in Sec 3, the displacements in Table 1 at surgical targets predicted by three methods, model-based approach and two non-rigid image registration techniques (ABA and Demon's)^{26, 33}, while showing magnitude similarities, exhibit different predicted shift directionality. The difference in the directionality of shift prediction from these methods may be attributed to different underlying principles employed by each method to generate the deformation field. Particularly, the presence of electrode leads shown on the registered iMR image in Fig 3(B) may introduce some local effects when non-rigid image registrations are performed, thus impacting the shift direction prediction. Nevertheless, while more understanding of the neuroanatomy is needed to match conditions, the results in Table 1 demonstrate considerable promise in that model predictions are on the correct scale.

5. CONCLUSIONS

A preliminary feasibility study is conducted using a biomechanical finite-element model-based brain shift correction strategy to predict intraoperative brain shift in DBS burr hole procedures with only sparse intraoperative data. Compared to approaches currently employed clinically to address the impact of brain shift, namely MER or iMR, the model-based approach has the potential to be a cost-effective complementary or alternative technology that presents minimal disruption to existing clinical workflow and infrastructure, which can be beneficial in aiding surgical navigation as well as providing accurate stimulation targeting, hence ensuring optimal DBS treatment quality. Yet important works still remain in qualifying the sparse intraoperative data to drive model correction. Here, sparse surface data was used but ultimately this was derived from iMR data. Typically, this data would not be available in medical centers not specialized in this manner. There may be options with recent advances in intraoperative imaging approaches such as CT and/or US. Refinement of the brain shift correction algorithm is also needed to better account for lateral shift components. In addition, clearly a larger study with more patients is needed to better assess the model-correction strategy. The important contribution of this work is the demonstration that with only a sparse set of data, reasonable approximations to electrode shift should be predictable.

ACKNOWLEDGEMENT

The rigid and non-rigid registration software was provided by Dr. Benoit Dawant. This work is supported by the National Institutes of Health, the National Institute for Neurological Disorders and Stroke, R01NS049251.

REFERENCES

1. M. S. Okun, and K. D. Foote, "Parkinson's disease DBS: what, when, who and why? The time has come to tailor DBS targets," *Expert Rev. Neurother.* **10**(12), 1847-1857 (2010).
2. M. S. Okun "Deep-Brain Stimulation for Parkinson's Disease," *New England Journal of Medicine* **367**(16), 1529-1538 (2012).
3. G. Deuschl, S. Paschen, and K. Witt, "Chapter 10 - Clinical outcome of deep brain stimulation for Parkinson's disease," in *Handbook of Clinical Neurology* A. M. Lozano, and M. Hallett, Eds., pp. 107-128, Elsevier (2013).
4. A. L. Benabid, "Deep brain stimulation for Parkinson's disease," *Curr. Opin. Neurobiol.* **13**(6), 696-706 (2003).
5. S. Miocinovic, S. Somayajula, S. Chitnis, and J. L. Vitek, "History, Applications, and Mechanisms of Deep Brain Stimulation," *JAMA Neurol.* **70**(2), 163-171 (2013).
6. P. Hickey, and M. Stacy, "Deep Brain Stimulation: A Paradigm Shifting Approach to Treat Parkinson's Disease," *Front. Neurosci.* **10**(11) (2016).
7. P. J. Slotty, M. A. Kamp, C. Wille, T. M. Kinfe, H. J. Steiger, and J. Vesper, "The impact of brain shift in deep brain stimulation surgery: observation and obviation," *Acta Neurochir.* **154**(11), 2063-2068 (2012).
8. J. L. Ostrem, N. Ziman, N. B. Galifianakis, P. A. Starr, M. San Luciano, M. Katz, C. A. Racine, A. J. Martin, L. C. Markun, and P. S. Larson, "Clinical outcomes using ClearPoint interventional MRI for deep brain stimulation lead placement in Parkinson's disease," *J. Neurosurg.* **124**(4), 908-916 (2016).
9. M. F. Khan, K. Mewes, R. E. Gross, and O. Skrinjar, "Assessment of brain shift related to deep brain stimulation surgery," *Stereotact. Funct. Neurosurg.* **86**(1), 44-53 (2008).
10. M. E. Ivan, J. Yarlagadda, A. P. Saxena, A. J. Martin, P. A. Starr, W. K. Sootsman, and P. S. Larson, "Brain shift during bur hole-based procedures using interventional MRI," *J. Neurosurg.* **121**(1), 149-160 (2014).
11. W. Thevathasan, and R. Gregory, "Deep brain stimulation for movement disorders," *Practical Neurology* **10**(1), 16 (2010).
12. R. Balachandran, J. E. Mitchell, B. M. Dawant, and J. M. Fitzpatrick, "Accuracy Evaluation of microTargeting Platforms for Deep-Brain Stimulation Using Virtual Targets," *IEEE Trans. Biomed. Eng.* **56**(1), 37-44 (2009).
13. M. L. Bootin, "Deep Brain Stimulation: Overview And Update," *Journal of Clinical Monitoring and Computing* **20**(5), 341-346 (2006).
14. D. Winkler, M. Tittgemeyer, J. Schwarz, C. Preul, K. Strecker, and J. Meixensberger, "The first evaluation of brain shift during functional neurosurgery by deformation field analysis," *J. Neurol. Neurosurg. Psychiatry* **76**(8), 1161-1163 (2005).

15. Y. Miyagi, F. Shima, and T. Sasaki, "Brain shift: an error factor during implantation of deep brain stimulation electrodes," *J. Neurosurg.* **107**(5), 989-997 (2007).
16. W. J. Elias, K. M. Fu, and R. C. Frysinger, "Cortical and subcortical brain shift during stereotactic procedures," *J. Neurosurg.* **107**(5), 983-988 (2007).
17. S. C. LaHue, J. L. Ostrem, N. B. Galifianakis, M. San Luciano, N. Ziman, S. Wang, C. A. Racine, P. A. Starr, P. S. Larson, and M. Katz, "Parkinson's disease patient preference and experience with various methods of DBS lead placement," *Parkinsonism & Related Disorders* **41**(25-30) (2017).
18. S. Pallavaram, B. M. Dawant, M. S. Remple, J. S. Neimat, C. Kao, P. E. Konrad, and P. F. D'Haese, "Effect of brain shift on the creation of functional atlases for deep brain stimulation surgery," *Int. J. Comput. Assist. Radiol. Surg.* **5**(3), 221-228 (2010).
19. K. J. Burchiel, S. McCartney, A. Lee, and A. M. Raslan, "Accuracy of deep brain stimulation electrode placement using intraoperative computed tomography without microelectrode recording Clinical article," *J. Neurosurg.* **119**(2), 301-306 (2013).
20. P. S. Larson, J. T. Willie, S. Vadivelu, H. Azmi-Ghadimi, A. Nichols, L. L. Fauerbach, H. B. Johnson, and D. Graham, "MRI-guided stereotactic neurosurgical procedures in a diagnostic MRI suite: Background and safe practice recommendations," *Journal of Healthcare Risk Management* **37**(1), 31-39 (2017).
21. J. M. Sullivan, G. Charron, and K. D. Paulsen, "A three-dimensional mesh generator for arbitrary multiple material domains," *Finite Elem. Anal. Des.* **25**(3-4), 219-241 (1997).
22. P. Dumpuri, R. C. Thompson, B. M. Dawant, A. Cao, and M. I. Miga, "An atlas-based method to compensate for brain shift: preliminary results," *Med Image Anal* **11**(2), 128-145 (2007).
23. K. Sun, T. S. Pheiffer, A. L. Simpson, J. A. Weis, R. C. Thompson, and M. I. Miga, "Near Real-Time Computer Assisted Surgery for Brain Shift Correction Using Biomechanical Models," *IEEE J Transl Eng Health Med* **2**((2014).
24. I. Chen, A. M. Coffey, S. Ding, P. Dumpuri, B. M. Dawant, R. C. Thompson, and M. I. Miga, "Intraoperative brain shift compensation: accounting for dural septa," *IEEE Trans Biomed Eng* **58**(3), 499-508 (2011).
25. F. Maes, A. Collignon, D. Vandermeulen, G. Marchal, and P. Suetens, "Multimodality image registration by maximization of mutual information," *IEEE Trans. Med. Imaging* **16**(2), 187-198 (1997).
26. G. K. Rohde, A. Aldroubi, and B. M. Dawant, "The adaptive bases algorithm for intensity-based nonrigid image registration," *IEEE Trans Med Imaging* **22**(11), 1470-1479 (2003).
27. I. Chen, A. L. Simpson, K. Sun, R. C. Thompson, and M. I. Miga, "Sensitivity analysis and automation for intraoperative implementation of the atlas-based method for brain shift correction," in *Proceedings of SPIE, Conference on Medical Imaging - Image-Guided Procedures, Robotic Interventions, and Modeling* (2013).
28. F. Lalys, C. Haegelen, T. D'Albis, and P. Jannin, "Analysis of electrode deformations in deep brain stimulation surgery," *Int. J. Comput. Assist. Radiol. Surg.* **9**(1), 107-117 (2014).
29. M. I. Miga, K. D. Paulsen, J. M. Lemery, S. D. Eisner, A. Hartov, F. E. Kennedy, and D. W. Roberts, "Model-updated image guidance: Initial clinical experiences with gravity-induced brain deformation," *IEEE Trans. Med. Imaging* **18**(10), 866-874 (1999).
30. D. R. Lynch, *Numerical partial differential equations for environmental scientists and engineers : a first practical course*, Springer, New York (2005).
31. K. D. Paulsen, M. I. Miga, F. E. Kennedy, P. J. Hoopes, A. Hartov, and D. W. Roberts, "A computational model for tracking subsurface tissue deformation during stereotactic neurosurgery," *IEEE Trans. Biomed. Eng.* **46**(2), 213-225 (1999).
32. A. Fedorov, R. Beichel, J. Kalpathy-Cramer, J. Finet, J. C. Fillion-Robin, S. Pujol, C. Bauer, D. Jennings, F. Fennessy, M. Sonka, J. Buatti, S. Aylward, J. V. Miller, S. Pieper, and R. Kikinis, "3D Slicer as an image computing platform for the Quantitative Imaging Network," *Magn Reson Imaging* **30**(9), 1323-1341 (2012).
33. X. Pennec, P. Cachier, and N. Ayache, "Understanding the "Demon's Algorithm": 3D non-rigid registration by gradient descent," *Medical Image Computing and Computer-Assisted Intervention, Miccai'99, Proceedings* **1679**(597-605) (1999).
34. C. H. Halpern, S. F. Danish, G. H. Baltuch, and J. L. Jaggi, "Brain shift during deep brain stimulation surgery for Parkinson's disease," *Stereotact. Funct. Neurosurg.* **86**(1), 37-43 (2008).
35. T. Obuchi, Y. Katayama, K. Kobayashi, H. Oshima, C. Fukaya, and T. Yamamoto, "Direction and Predictive Factors for the Shift of Brain Structure During Deep Brain Stimulation Electrode Implantation for Advanced Parkinson's Disease," *Neuromodulation* **11**(4), 302-310 (2008).